# NAADP-mediated $Ca^{2+}$ signaling via type 1 ryanodine receptor in T cells revealed by a synthetic NAADP antagonist

Werner Dammermann[a,1], Bo Zhang[b,1], Merle Nebel[a,1], Chiara Cordiglieri[c,1], Francesca Odoardi[c,d], Tanja Kirchberger[a], Naoto Kawakami[c], James Dowden[b], Frederike Schmid[a], Klaus Dornmair[e], Martin Hohenegger[f], Alexander Flügel[c,d,g,1], Andreas H. Guse[a,1], and Barry V. L. Potter[b,1,2]

[a]The Calcium Signaling Group, University Medical Centre Hamburg-Eppendorf, Centre of Experimental Medicine, Institute of Biochemistry and Molecular Biology I: Cellular Signal Transduction, 20246 Hamburg, Germany; [b]Wolfson Laboratory of Medicinal Chemistry, Department of Pharmacy and Pharmacology, University of Bath, Bath, BA2 7AY, United Kingdom; [c]Department of Neuroimmunology, Max Planck Institute for Neurobiology, 82152 Martinsried, Germany; [d]Institute for Multiple Sclerosis Research, Gemeinnützige Hertie-Stiftung and University Medical Centre Göttingen, 37073 Göttingen, Germany; [e]Institute for Clinical Neuroimmunology, Ludwig Maximilians University, 82152 Martinsried, Germany; [f]Institute of Pharmacology, Medical University of Vienna, 1090 Vienna, Austria; and [g]Institute for Immunology, Ludwig Maximilians University, 80336 Munich, Germany

Edited by David E. Clapham, Harvard Medical School, Boston, MA, and approved May 5, 2009 (received for review October 8, 2008)

**The nucleotide NAADP was recently discovered as a second messenger involved in the initiation and propagation of $Ca^{2+}$ signaling in lymphoma T cells, but its impact on primary T cell function is still unknown. An optimized, synthetic, small molecule inhibitor of NAADP action, termed BZ194, was designed and synthesized. BZ194 neither interfered with $Ca^{2+}$ mobilization by D-*myo*-inositol 1,4,5-trisphosphate or cyclic ADP-ribose nor with capacitative $Ca^{2+}$ entry. BZ194 specifically and effectively blocked NAADP-stimulated [$^3$H]ryanodine binding to the purified type 1 ryanodine receptor. Further, in intact T cells, $Ca^{2+}$ mobilization evoked by NAADP or by formation of the immunological synapse between primary effector T cells and astrocytes was inhibited by BZ194. Downstream events of $Ca^{2+}$ mobilization, such as nuclear translocation of ''nuclear factor of activated T cells'' (NFAT), T cell receptor-driven interleukin-2 production, and proliferation in antigen-experienced $CD4^+$ effector T cells, were attenuated by the NAADP antagonist. Taken together, specific inhibition of the NAADP signaling pathway constitutes a way to specifically and effectively modulate T-cell activation and has potential in the therapy of autoimmune diseases.**

antagonism | nucleotide | second messenger | synthesis

$Ca^{2+}$ signaling is one of the essential signal transduction systems involved in T-cell activation. Upon formation of immunological synapses, a complex network of $Ca^{2+}$ signaling modules is activated in a spatiotemporal fashion. One of the major mechanisms involved, capacitative $Ca^{2+}$ entry via Orai1/CRACM1 (1–4), requires continuous $Ca^{2+}$ release from intracellular pools for activation. Besides $Ca^{2+}$ release by D-*myo*-inositol 1,4,5-trisphosphate ($InsP_3$, ref. 5), we have shown that two additional second messengers, cyclic ADP-ribose (cADPR; ref. 6) and NAADP (Fig. 1*A*; refs. 7–10) are critically involved in the process of $Ca^{2+}$ release in T cells.

NAADP was discovered by Lee and coworkers as an impurity in nicotinamide adenine dinucleotide phosphate (NADP) preparations and is the most powerful endogenous $Ca^{2+}$ mobilizing compound known to date (11). Both plant and animal cells have been shown to respond to application of NAADP (reviewed in refs. 12–14). A limited number of reports demonstrated that extracellular stimulation increased intracellular NAADP concentrations, being in accordance with a second messenger function for NAADP (reviewed in refs. 15–17).

A controversial issue regarding NAADP is the molecular identity of its receptor. Clearly, in sea urchin eggs, the characterization of NAADP induced $Ca^{2+}$ release revealed that a receptor/channel different from the $InsP_3$ receptor or the ryanodine receptor (RyR) is involved (11, 18). In addition, Lee's group obtained evidence for a non-ER $Ca^{2+}$ store sensitive to NAADP in stratified sea urchin eggs (19) that was finally identified as a lysosomal compartment (20–23). Recent evidence indicates that the novel NAADP receptor on lysosomes is the $Ca^{2+}$ channel transient receptor potential, mucolipin 1 (TRP-ML1; 24, 25). In contrast, data obtained by reconstitution of RyR in artificial bilayers suggest direct activation of RyR by NAADP (26, 27). In addition, NAADP-induced $Ca^{2+}$ signaling involving RyR was described for MIN6 cells (28), pancreatic acinar cells (29, 30), and human T cells (9, 10). In contrast to the lysosomal store mentioned above, in those cells where RyR involvement was demonstrated, the $Ca^{2+}$ pool sensitive to NAADP appears to be the SR/ER or ER-related membrane systems like the nuclear envelope rather than lysosomes (26, 27, 29, 31).

Over the last years, some of us have analyzed the NAADP pathway in Jurkat T lymphocytes in detail, including formation of NAADP (8), local and global $Ca^{2+}$ release via RyR (9, 10), and identification of the NAADP sensitive $Ca^{2+}$ store residing within the ER (31). However, the functional role of NAADP in primary T cells has remained unclear due to the inability to specifically interfere with this signaling pathway by means of chemical biological tools. Here we report the synthesis and biological characterization of an optimized NAADP antagonist for T cells, termed BZ194.

## Results

**A NAADP Antagonist Based on Nicotinic Acid.** Microinjection of NAADP into single Jurkat T cells induced robust $Ca^{2+}$ signaling as described previously (7, 9, 10, 31). Co-injection of nicotinic acid, but not of nicotinamide, greatly reduced $Ca^{2+}$ signaling induced by NAADP (Fig. 1*B*), indicating that nicotinic acid derivatives might be suitable for chemical biological intervention as NAADP antagonists and for possible drug design. Since NAADP is highly active in $Ca^{2+}$ release, while the structurally related parent compound NADP (Fig. 1*A*) is inactive (11), it is very likely to be the nicotinic acid moiety that interferes with NAADP-mediated $Ca^{2+}$ signaling. Indeed, since cellular uptake of the polar nicotinic acid is slow and

Author contributions: A.F., A.H.G., and B.V.L.P. designed research; W.D., B.Z., M.N., C.C., F.O., T.K., N.K., J.D., F.S., K.D., and M.H. performed research; and M.H., A.F., A.H.G., and B.V.L.P. wrote the paper.

The authors declare no conflict of interest.

This article is a PNAS Direct Submission.

Freely available online through the PNAS open access option.

[1]W.D., B.Z., M.N., C.C., A.F., A.H.G., and B.V.L.P. contributed equally to this work.

[2]To whom correspondence should be addressed at: Wolfson Laboratory of Medicinal Chemistry, Department of Pharmacy and Pharmacology, University of Bath, Bath BA2 7AY, United Kingdom. E-mail: b.v.l.potter@bath.ac.uk.

This article contains supporting information online at www.pnas.org/cgi/content/full/0809997106/DCSupplemental.

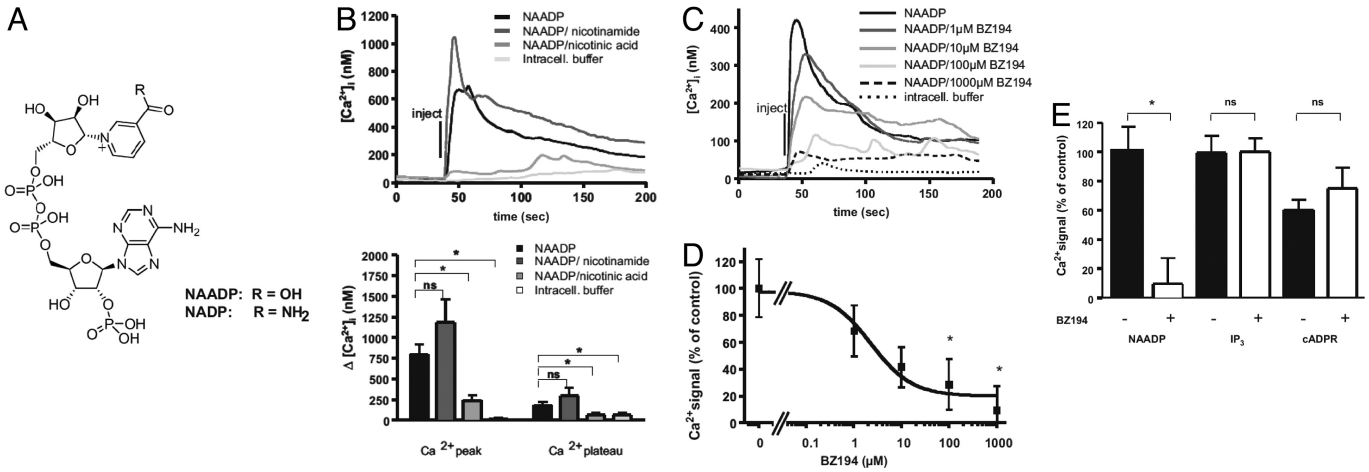


**Fig. 1.** Nicotinic acid and its derivative BZ194 inhibit NAADP-mediated $Ca^{2+}$ signaling in T cells. (*A*) Structures of NAADP and NADP. (*B*) NAADP-induced $Ca^{2+}$ signaling in T cells is inhibited by nicotinic acid. Jurkat T cells were loaded with Fura-2/AM and were microinjected with 100 nM NAADP, 100 nM NAADP plus 1 mM nicotinamide, or 100 nM NAADP plus 1 mM nicotinic acid, or intracellular buffer. Free cytosolic $Ca^{2+}$ ($[Ca^{2+}]_i$) was measured. Mean data of 4–12 experiments are shown (*Upper*). The bar chart (*Lower*) summarizes the data ($Ca^{2+}$ peak and $Ca^{2+}$ plateau; means ± SEM., $n = 4 - 12$; *, $P \leq 0.05$; ns, not significant). (*C*) Inhibition of NAADP-induced $Ca^{2+}$ signaling upon co-injection with BZ194. Jurkat T cells were co-injected with 100 nM NAADP and increasing concentrations of BZ194. Mean data of 5–13 experiments are shown. (*D*) Concentration-response curve of NAADP-induced $Ca^{2+}$ signaling upon microinjection with BZ194 (mean ± SEM, $n = 5–13$; *, $P \leq 0.05$). (*E*) BZ194 does not directly interfere with $InsP_3$- or cADPR-mediated $Ca^{2+}$ release. Jurkat T cells were loaded with Fura2/AM. Thereafter, single cells were co-injected with 1 mM BZ194 and either NAADP (100 nM), $InsP_3$ (4 $\mu$M), or cADPR (100 $\mu$M), and $Ca^{2+}$ signaling was recorded. Relative values are shown as percentages of NAADP-induced $[Ca^{2+}]_i$. Data represent means ± SEM, $n = 5–13$; *, $P \leq 0.05$; ns, not significant.

this molecule is obviously intracellularly channeled into biosynthesis of nicotinamide adenine dinucleotide (NAD), we reasoned that design of a membrane-permeant analogue should be a powerful approach toward targeting the NAADP/$Ca^{2+}$ signaling pathway. NAADP itself is clearly too polar to be a useful starting point for any chemical design, but the nicotinic acid moiety is ideally based from which to develop modified drug-like small molecule NAADP modulators. Consequently, prototype nicotinic acid derivatives were synthesized by alkylation of nicotinic acid using 2-bromoacetylamides as the alkylating agents. From a library of alkylated nicotinic acid derivatives (representative examples are shown in Fig. S1*A*) the *N*-alkylated 8-carbon side chain derivative, 3-carboxyl-1-octylcarbamoylmethyl-pyridinium (BZ194) emerged as a potent antagonist of proliferation of effector T cells (Fig. S1*B*). Importantly, when BZ194 was co-injected into Jurkat T cells together with NAADP, both the initial $Ca^{2+}$ peak and the sustained $Ca^{2+}$ plateau observed upon injection of NAADP were concentration-dependently blocked resulting in an $IC_{50}$ in the low micromolar range (Fig. 1 *C* and *D*). Notably, BZ194 co-injected together with the $Ca^{2+}$ mobilizing second messengers $InsP_3$ or cADPR (Fig. 1*E* and Fig. S2 *A* and *B*) did not inhibit their activity suggesting high specificity of BZ194 toward the NAADP/$Ca^{2+}$ signaling pathway.

**RyR1 Activation by NAADP.** Previously, we have presented evidence for NAADP targeting the RyR (9, 10), including use of single channel recordings (26). To extend these results, we used highly purified RyR1 (Fig. 2*A*), and analyzed high-affinity [$^3$H]ryanodine binding, which is proportional to channel opening (32). NAADP significantly accelerated the association of [$^3$H]ryanodine to the purified RyR1 (Fig. 2*B*). While BZ194 had no effect on the basal [$^3$H]ryanodine binding, the NAADP-induced increment in radioligand binding was completely abrogated. Importantly, the dissociation of [$^3$H]ryanodine was not influenced by BZ194 (Fig. 2*C*) whereas the dissociation from NAADP preactivated RyR1 was significantly accelerated, indicating an allosteric regulation. The basal equilibrium binding was not significantly altered by increasing concentrations of BZ194 (Fig. 2*D*). However, [$^3$H]ryanodine binding stimulated by NAADP was antagonized by BZ194 in a concentration-dependent manner (Fig. 2*D*). The $IC_{50}$ value was comparable with that observed for $Ca^{2+}$ release inhibition in the native cellular system (Fig. 1*D*). Hence, these results are indicative of direct targeting of RyR1 by both NAADP and BZ194.

**Antagonism of $Ca^{2+}$ Signaling in Primary T Cells by NAADP Antagonist BZ194.** Having demonstrated specific antagonism of NAADP effects at the purified RyR1 and in the model T cell line Jurkat, primary myelin-basic-protein-reactive rat T cells ($T_{MBP}$ cells) were used to study the role of NAADP activation in effector T cells. $T_{MBP}$ cells express both RyR1 and RyR3, although RyR3 to a lesser extent (Fig. 3*A*). RyR1 showed a significant co-localization with an ER marker, while RyR2 was not detected (Fig. 3*A*).

BZ194-type compounds with varying lengths and types of side chains R1 and/or R2 (Fig. S1*A*), were tested with intact $T_{MBP}$ cells using antigen-induced proliferation as read-out (Fig. S1*B*). Using iterative exploration of substituents the single octyl side chain of BZ194 proved to be most suitable for membrane permeability and neither a longer side chain, for example, 10 carbon atoms in BZ71, nor a lack of side chain in CMA008 had any effect on $T_{MBP}$ cell proliferation (Fig. S1*A* and *B*). Interestingly, the other active analog identified, the disubstituted BZ52, possesses the same number of side chain carbon atoms, but distributed over 2 centers. BZ194 blocked $Ca^{2+}$ signaling in intact $T_{MBP}$ cells upon stimulation with the specific antigen. Using astrocytes pulsed with MBP, $Ca^{2+}$ signaling was recorded upon formation of the immunological synapse (Fig. 3*B*). While presentation of MBP by the astrocytes resulted in substantial $Ca^{2+}$ signaling, reaching a plateau phase within about 4 min, BZ194 significantly diminished this response (Fig. 3 *B* and *C*). Analysis on a single-cell level revealed that treatment with BZ194 significantly decreased the percentage of T cells showing high $Ca^{2+}$ responses. With MBP as antigenic protein, 21 out of 30 cells showed $Ca^{2+}$ signals >200 nM, whereas upon BZ194 preincubation $Ca^{2+}$ signals >200 nM were observed in only 17 out of 31 cells. If only $Ca^{2+}$ signals >300 nM were taken into account, with MBP as antigenic protein, 19 out of 30 cells responded, while BZ194 decreased the number of responding cells to 10 out of 31. $Ca^{2+}$ signaling of $T_{MBP}$ cells evoked by anti-CD3

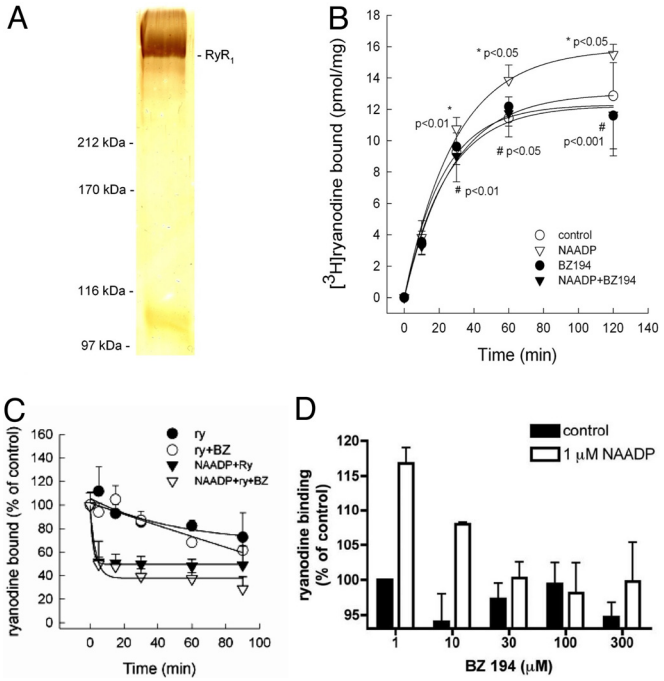


**Fig. 2.** Targeting of NAADP RyR1 interaction by BZ194. (*A*) Silver-stained gel demonstrating the purity of RyR1 preparation. (*B*) Kinetics of NAADP-induced association of [$^3$H] ryanodine to the purified RyR1 at 30 °C. Specific [$^3$H]ryanodine binding in the absence (control) or presence of 300 nM NAADP; BZ194 (100 $\mu$M) was combined with both control and NAADP experiments. Asterisk (*) denotes statistical significance of NAADP over control, cross (#) that of BZ194 plus NAADP over NAADP alone. Data are mean ± SD. ($n$ = 4). (*C*) After 2 h of association, dissociation of bound [$^3$H] ryanodine (20 nM) was triggered by 20 $\mu$M cold ryanodine (ry) in the absence or presence of 300 nM NAADP or 100 $\mu$M BZ194 (BZ) at 30 °C. Data are mean ± SD. ($n$ = 4). (*D*) Inhibition of NAADP-stimulated [$^3$H]ryanodine binding to RyR1 by increasing concentrations of BZ194 after 2 h at 30 °C. Data are mean ± SEM ($n$ = 2–14).

monoclonal antibody, and subsequent crosslinking of the primary antibody was also sensitive to BZ194. Both the initial $Ca^{2+}$ peak and the sustained $Ca^{2+}$ plateau were reduced in a concentration-dependent fashion with the plateau being more sensitive compared with the initial peak (Fig. 3 *D* and *E*). The antagonistic effect of BZ194 required preincubation periods (Fig. 3*F*), indicating moderate membrane permeancy and/or activation of drug export systems.

Capacitative $Ca^{2+}$ entry was not inhibited by BZ194 since $Ca^{2+}$ signaling induced by thapsigargin in $T_{MBP}$ cells was unaffected (Fig. 3 *G* and *H*). Taken together, our data suggest a crucial role for NAADP as trigger of $Ca^{2+}$ signals during the process of immunological synapse formation.

**NAADP Antagonist BZ194 Suppressed Downstream Events of $Ca^{2+}$ Signaling.** Calcium signaling in T cells activates $Ca^{2+}$/calmodulin dependent phosphatase calcineurin leading to "nuclear factor of T cells" (NFAT) dephosphorylation and translocation into the nucleus. BZ194 significantly reduced nuclear translocation of NFAT following combined stimulation of rat $T_{MBP}$ cells with anti-CD3 and anti-CD28 antibodies (Fig. 4 *A* and *B*).

Furthermore, BZ194 efficiently suppressed antigen-induced production of the major T cell cytokine IL-2, as determined on the mRNA and protein levels (Fig. 4 *C* and *D*). Importantly, BZ194-mediated regulation of IL-2 levels was reversible. Re-stimulation of the suppressed T cells in the absence of BZ194 led to complete reconstitution of the original cytokine profile (Fig. S3). In a similar fashion as for rat T cells, in human MBP-specific T-cell clones a decrease in IL-2 mRNA, IL-2 production and proliferation was observed upon preincubation with BZ194 (Fig. S4).

The NAADP antagonist suppressed antigen-induced T-cell proliferation at concentrations higher than 50 $\mu$M. As expected, the highly polar and membrane impermeable parent compound nicotinic acid was ineffective (Fig. S1*B*). Non-stimulated $T_{MBP}$ cells tolerated prolonged treatment (48 h) with BZ194; furthermore, T cells which had previously been suppressed by BZ194 remained responsive to their antigen, when re-challenged with antigen-pulsed, antigen-presenting cells (APCs) after wash-out of BZ194 (Fig. S5). Moreover, BZ194 treatment 48 h after stimulation did not impair T-cell proliferation and did not induce increased cell death (Fig. S5). Together with the microinjection (Fig. 1 *B–E*) and the [$^3$H]ryanodine binding results (Fig. 2), these data indicate very specific targeting of RyR1 since (*i*) wash-out of BZ194 reverted the inhibition, and (*ii*) late stages of T-cell activation (>48h) were unaffected by addition of BZ194. This interpretation was further substantiated by directly demonstrating that BZ194 did not affect cellular signaling cascades beyond $Ca^{2+}$ signaling. Bypassing early $Ca^{2+}$ signaling by stimulating $T_{MBP}$ cells with $Ca^{2+}$ ionophore ionomycin either in combination with anti-CD3/anti-CD28 antibodies or with phorbol ester (PMA) rendered the T cells non-susceptible to BZ194 inhibition (Fig. 4*E*). Similar inhibition of proliferation by BZ194 treatment was observed in ovalbumin and S100$\beta$-specific rat T cells (Fig. S6).

## Discussion

Recent reports on the role of $Ca^{2+}$ signaling in activation of T cells indicate a complex network involving NAADP as initial $Ca^{2+}$ trigger (7–10, reviewed in ref. 17). Here we report that the nicotinic acid residue of NAADP is suitable as a starting point for the development of NAADP antagonists. In sea urchin eggs, the 2′-phospho-group of the ribose bound to the adenine-linked ribose, the 6-$NH_2$ group of adenine and the nicotinic acid moiety were identified as important structural elements for $Ca^{2+}$ release (33). Since these 3 structural moieties are distributed over the whole NAADP molecule, it was deemed very difficult to design a potential antagonist molecule comprising alterations in all 3 structural elements. Thus, we started with simple *N*-alkylated analogues of nicotinic acid to which lipophilic groups to enhance membrane permeability were covalently bound. Additionally, we explored other substitutions around the aromatic nucleus to optimize activity. A range of potential ligands was synthesized to gain the optimal balance between cellular permeability, activity, and physicochemical properties. In structure-activity studies, we found that little variation beyond a moderate-sized hydrophobic side chain was tolerated by T cells. In fact, the 8 carbon-side chain analog BZ194 was effective with an $IC_{50}$ around 100 $\mu$M. This extra hydrophobicity in BZ194 can also be distributed over 2 substituents on nitrogen atoms giving a similar effect in BZ52 and thus is consistent without further optimization. In contrast to BZ194 and BZ52, BZ23, an analog with a substituted aromatic side chain, enhanced proliferation of $T_{MBP}$ cells. The molecular mechanism underlying this interesting observation will be the subject of further experiments.

One obvious concern in using pharmacological compounds is the question of their specificity. To this end, we excluded that BZ194 affects the other known $Ca^{2+}$-mobilizing pathways, that is $InsP_3$- or cADPR-dependent $Ca^{2+}$ release, or capacitative $Ca^{2+}$ entry. Furthermore, (*i*) bypassing inhibition of NAADP signaling by $Ca^{2+}$ ionophore, (*ii*) reversibility of inhibition of proliferation upon wash-out of BZ194, and (*iii*) lack of effect of BZ194 addition at later time points of T-cell activation altogether strongly suggest high specificity of the drug used. Finally, we also ensured that BZ194 does not block physiological $Ca^{2+}$ signaling via different mechanisms in other cell types, for example, in electrically paced mouse cardiac myocytes or human HeLa cells stimulated via G protein coupled muscarinic acetylcholine receptors.

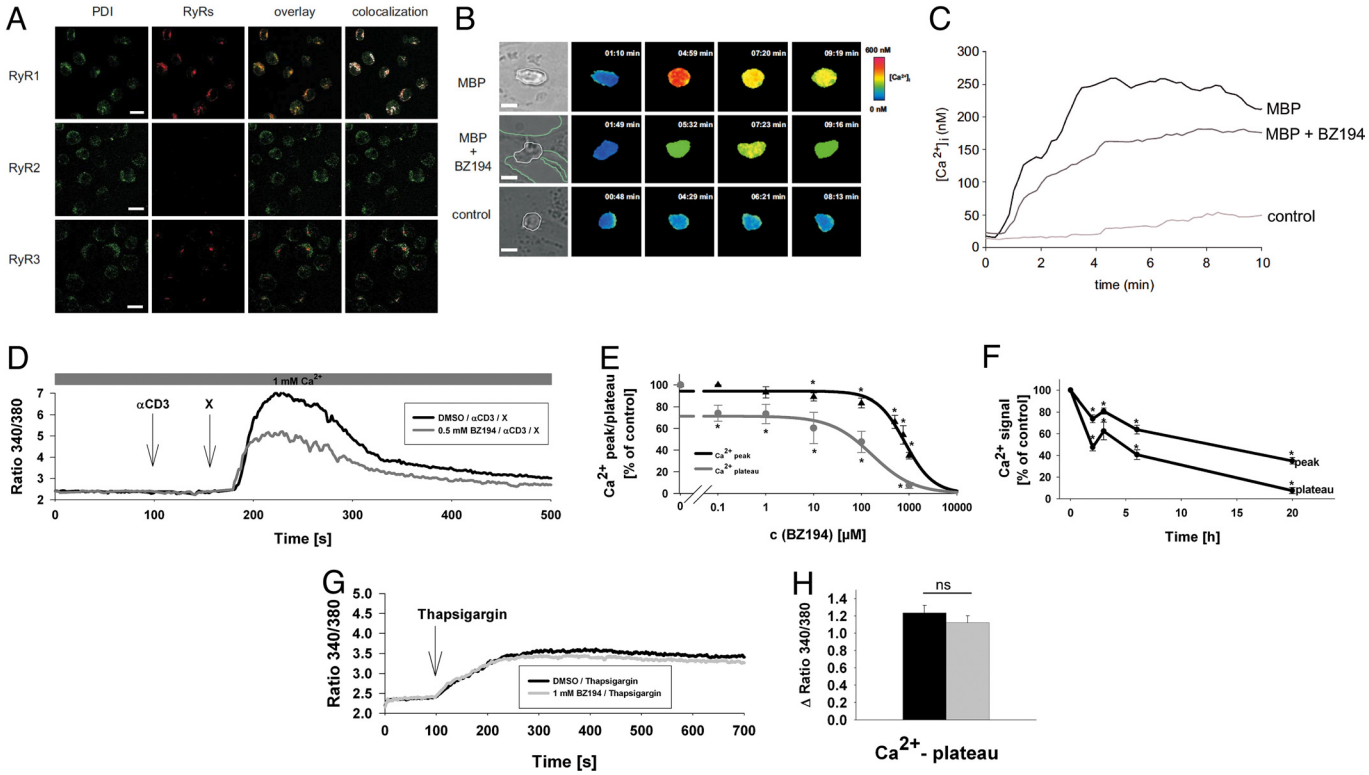


**Fig. 3.** RyR expression and antagonism of $Ca^{2+}$ signaling in rat MBP-specific effector T cells. (*A*) Expression of RyR subtypes in effector T cells. Immunofluorescence for RyR1 to 3 (red) and the endoplasmatic reticulum marker protein disulphide isomerase (PDI, green). (Scale bar, 10 $\mu$m.) (*B*) Suppression of $Ca^{2+}$ signaling in Fura2-loaded $T_{MBP}$ cells stimulated in the presence of MBP-pulsed astrocytes. Rat F10 astrocytes with up-regulated MHC II expression were pulsed with MBP. $T_{MBP}$ cells, either preincubated with BZ194 (2 mM, MBP + BZ194) or left untreated (MBP), were loaded with Fura-2/AM and added to the astrocytes. In control experiments, astrocytes were not pulsed with MBP (control). Time point 0 was defined as first visible contact between a T cell and an astrocyte. $Ca^{2+}$ imaging was performed as detailed in *SI Methods*. (*B*) shows a representative experiment with T cells highlighted by white lines in the brightfield images. (Scale bar, 5 $\mu$m.) (*C*) Mean global $[Ca^{2+}]_i$ data from 14 (control: no MBP), 30 (MBP pulsed astrocytes), or 31 (MBP pulsed astrocytes plus T cells preincubated with BZ194) T cells are displayed. (*D*) Resting rat $T_{MBP}$ cells were loaded with Fura2/AM and cell suspension measurements were carried out as described in Methods. Arrows indicate the addition of $\alpha$CD3 or crosslinking (X) antibodies. Cells were preincubated with 500 $\mu$M BZ194 overnight. (*E*) Concentration-response curves summarizing data from (*D*) (transient $Ca^{2+}$ peak and $Ca^{2+}$ plateau; mean ± SEM, $n = 8$–9). (*F*) Effect of BZ194 preincubation time on $Ca^{2+}$ signaling (mean ± SEM, $n = 8$–9). (*G*) Cells were preincubated with 1 mM BZ194 overnight and thapsigargin (1 mM, arrow) was added to induce capacitative $Ca^{2+}$ signaling; mean data ± SEM ($n = 9$) are summarized in *H*. *, $P \leq 0.05$ according to Student's *t* test; ns, not significant.

Recently, 1-carbamoylmethyl-3-carboxy pyridinium iodide (abbreviated CMA008; see Fig. S1 *A* and *B*) was shown to antagonize NAADP effects in sea urchin eggs and murine pancreatic acinar cells (34). Although this analog is structurally related to BZ194, no inhibitory activity in T cells was observed. This non-sensitivity of T cells vs. sensitivity of pancreatic acinar cells reflects the different nature of the target $Ca^{2+}$ store and the NAADP receptor involved. While a novel NAADP-sensitive channel has been proposed for those cell types with acidic stores sensitive to NAADP (20–25), strong evidence for RyR1 as NAADP target was obtained in T cells since NAADP modulated high-affinity [$^3$H]ryanodine binding. This in turn reflects RyR1 channel opening, as the radioligand binds to the open conformation of the ion channel (32, 35–37). Importantly, the BZ194 concentrations needed to suppress NAADP induced $Ca^{2+}$ release in Jurkat T lymphocytes (Fig. 1*D*) equal that needed to prevent NAADP stimulated [$^3$H]ryanodine binding (Fig. 2*B*). Thus, these data suggest that the RyR1 is the primary target for BZ194. RyR3 is expressed to a lesser extent in effector T cells. Gene silencing experiments in Jurkat T cells indicate that RyR3 is targeted by cADPR (38). However, defining the precise interaction between cADPR and any RyR subtype, as shown in Fig. 2 of this report for NAADP and highly purified RyR1, requires further extensive experiments. Alternatively proposed NAADP targets, such as TRP-ML 1 (24, 25) that are localized to lysosomes, do not appear to play a major role in T cells since the ER rather than lysosomes are involved in NAADP mediated $Ca^{2+}$ signaling in T cells (31).

The present study complements published models on temporal events of $Ca^{2+}$ release. We show here that NAADP via RyR1 activation acts as the initializing trigger, which controls further $Ca^{2+}$ release events by supplying local $Ca^{2+}$ signals for $Ca^{2+}$ induced $Ca^{2+}$ release to amplify $InsP_3$- and cADPR-induced $Ca^{2+}$ release. NAADP mediated $Ca^{2+}$ release starts rapidly within a few seconds upon TCR/CD3 ligation (8). By contrast, $InsP_3$- and cADPR-mediated releases appear within a few minutes (39) or within tens of minutes, respectively (6). A possible reason for this complex regulatory $Ca^{2+}$ release network may be the need for temporal checkpoints, at which the T cell, based upon the input via the TCR/CD3 complex and diverse co-receptors, can control whether to proceed with activation or not (40). The decision whether to continue or to stop $Ca^{2+}$ signaling may ultimately result in cell proliferation and exertion of effector functions, or it may drive the T cell into a state of unresponsiveness or cell death. The NAADP/$Ca^{2+}$ signaling pathway seems to control this decision, since expression of the major cytokine involved in T cell proliferation, IL-2, depends on a full, NAADP-initiated $Ca^{2+}$ response. If the NAADP pathway is blocked by specific inhibitors, $Ca^{2+}$ signaling is only partially activated. Therefore, it does not provide a sufficient long-lasting increase in the free cytosolic $Ca^{2+}$ concentration to allow $Ca^{2+}$/calmodulin- and calcineurin-dependent translocation of NFAT into the nucleus (41).

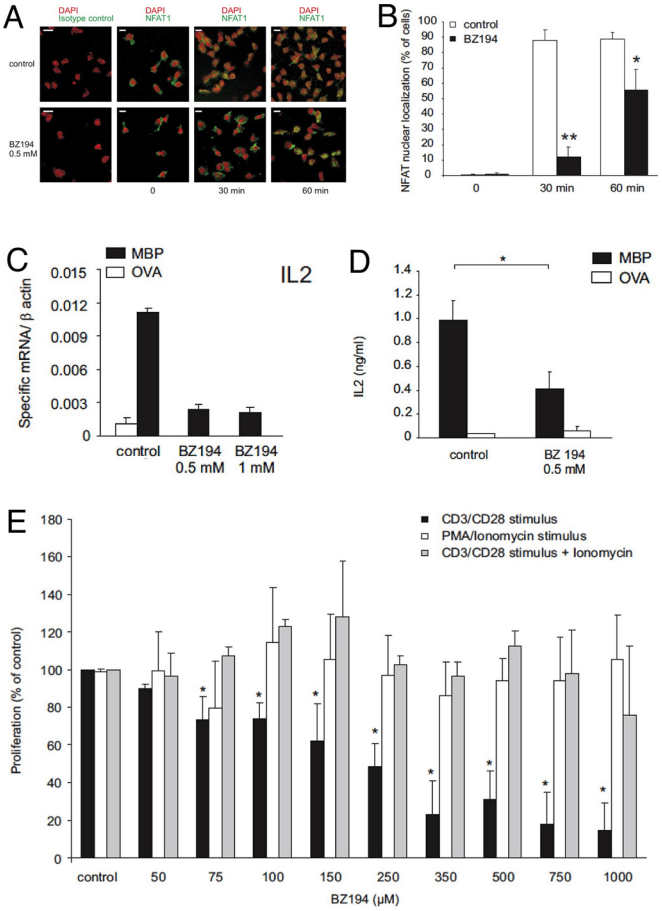


**Fig. 4.** NAADP signaling is essential for efficient activation of antigen-specific effector T cells. (*A*) BZ194 reduces NFAT-1 nuclear translocation. Immunocytochemistry of BZ194-treated or control (DMSO- treated) $T_{MBP}$ cells 0, 30, or 60 min after stimulation with αCD3/CD28 antibodies. Red, DAPI staining; green, NFAT-1 or isotype control staining. (Scale bars, 10 μm.) Representative data of 3 independent experiments are shown. (*B*) Quantification of NFAT-1 nuclear translocation, expressed as percent of cells. Values respresent means ± SD, data from 3 independent experiments including at least 150 cells per counting. *P* values: *, $P \leq 0.05$; **, $P \leq 0.01$. (*C–E*) BZ194 suppresses activation-induced IL-2 expression in rat and human $T_{MBP}$ cells. (*C*) Quantitative PCR of rat $T_{MBP}$ cells challenged with control antigen- (OVA, white) or MBP- (black) pulsed APCs in the presence of vehicle (control), 0.5 or 1 mM BZ194. mRNA was extracted 48 h after stimulation. Values are normalized to β actin mRNA. Representative data of 3 independent experiments are shown. All differences are statistically significant (*P* value, *P* at least ≤ 0.05). (*D*) IL-2 protein release of $T_{MBP}$ cells 48 h after stimulation, determined by ELISA. Values represent means ± SD of triplicate measurements. Representative data of at least 2 independent experiments are shown. *, $P \leq 0.0001$. (*E*) BZ194 blocks antigen-induced T cell proliferation, but does not interfere with T-cell activation cascades beyond $Ca^{2+}$ signaling. $T_{MBP}$ cells incubated with the indicated amounts of BZ194 were stimulated with αCD3/CD28 antibodies (black bars), PMA/ionomycin (white bars) or αCD3/CD28 antibodies + ionomycin (gray bars). $T_{MBP}$ cells reactivity was determined by [$^3$H]dT incorporation 2 d later. Proliferation is indicated as percent of control (no BZ194 treatment; CD3/CD28 stimulation: 6445 ± 475 cpm; CD3/CD28 + ionomycin stimulation: 6624 ± 320 cpm; PMA/ionomycin stimulation: 5264 ± 521cpm). Data represent means ± SD of measurements from 5 independent experiments. *, $P \leq 0.01$.

By establishing highly specific NAADP antagonists, we demonstrate here that the NAADP/$Ca^{2+}$ pathway is critically involved in early activation events of antigen-specific $CD4^+$ effector T cells. NAADP antagonist BZ194 blocked the NAADP stimulated RyR1 $Ca^{2+}$ release and, as a secondary and indirect effect, all downstream $Ca^{2+}$ signaling events depending on initial trigger $Ca^{2+}$ as co-agonist were diminished. Thereby, NAADP antagonist BZ194 specifically interfered with the interactions of effector T cells with APCs. Importantly, while down-modulating $Ca^{2+}$ signaling and effector reactions of T cells, BZ194 did not show any major unspecific effects. This may in part be explained by the virtual absence of effects of BZ194 on basal equilibrium [$^3$H]ryanodine binding or dissociation kinetics (Fig. 2). BZ194 is thus an inhibitor of the RyR1, which accesses the ion channel in the presence of NAADP, implying that channel opening is necessary for its inhibitory action. The fact that BZ194 had virtually no inhibitory effect on basal binding (Fig. 2 *B* and *D*) supports this assumption. In terms of potential clinical usage such a mechanism of action may result in less effects on the basal RyR1 activity, but increased inhibition if the RyR1 is activated. Thus, one may assume that side effects by such a mechanism of action could be reduced compared with a state-independent inhibitor of the RyR1.

Therefore, the involvement of the NAADP/$Ca^{2+}$ signaling pathway in a primary T-cell model relevant for the pathogenic context of T cell-mediated autoimmunity has been demonstrated in vitro using a purpose-designed and optimized synthetic small molecule antagonist. The use of such NAADP antagonists in the corresponding animal model of experimental autoimmune encephalomyelitis (EAE) is the subject of ongoing investigations. Treatment with BZ194 in vivo was found to significantly ameliorate clinical disease. Thus, this approach may result in additional therapeutic agents for treating autoimmune diseases such as multiple sclerosis.

## Methods

**Materials.** NAADP was supplied by Sigma. cADPR and $InsP_3$ were obtained from Biolog. All reagents and solvents were of commercial quality and were used directly unless otherwise described.

**Synthesis of 3-Carboxy-1-octylcarbamoylmethyl-pyridinium Bromide (BZ194).** For synthesis, nicotinic acid (1.62 mmol) and 2-bromo-*N*-octylacetamide (1.62 mmol) were dissolved in dry dimethylformamide (DMF, 4 mL) and the reaction solution was heated at 65 °C overnight in the dark. DMF was evaporated in vacuo and the resulting residue was dissolved in a small amount of methanol. The crude compound was precipitated by dropwise addition of ether. 3-Carboxy-1-octylcarbamoylmethylpyridinium was further purified by flash column chromatography (0–10% methanol against dichlormethane) and was crystallized in methanol and acetone. The compound exhibited spectroscopic and analytical properties commensurate with its structure using standard techniques as detailed in the *SI Methods*.

**High-Affinity [$^3$H]Ryanodine Binding.** RyR1 was purified from rabbit skeletal muscle (42). Purity of the RyR1 preparation was controlled by SDS/PAGE and silver staining (43). High-affinity [$^3$H]ryanodine binding was carried out with 7.5–20 μg purified RyR1, which was incubated for the indicated times at 30 °C in a buffer containing 20 mM Hepes (pH 7.4), 140 mM KCl, 50 mM NaCl, 2.5% phosphatidyl choline, 7 mM CHAPS, and 20 nM [$^3$H]ryanodine supplemented by protease inhibitors (1 μM leupeptin, 1 μM aprotinin, and 100 μM Pefablock). The free calcium concentration was adjusted to 6 μM by ratio of $CaCl_2$ and EGTA. The reactions were terminated by filtration. Specific binding was determined by subtraction of nonspecific binding in the presence of 20 μM ryanodine (42).

**Generation and Culturing of T Cells.** Jurkat lymphoma T cells (clone JMP) were cultured as described previously (43). Rat antigen-specific T cell clones were obtained from lymph node preparations of immunized Lewis rats. Stimulation, expansion, and culture of specific rat T cells were conducted under conditions as described (44). Details concerning generation of MBP-specific $CD4^+$ T cells ($T_{MBP}$) retrovirally engineered to express the marker gene EGFP are provided in the *SI Methods*.

**Cytosolic $Ca^{2+}$ Measurements.** Both Jurkat T lymphoma and rat $T_{MBP}$ cells were loaded with Fura-2/AM (Calbiochem) as described (44) and kept in the dark at room temperature until use. Intracellular $Ca^{2+}$ ($[Ca^{2+}]_i$) was determined in suspensions of Fura-2-loaded rat $T_{MBP}$ cells which had been preincubated with BZ194 or DMSO at the indicated concentrations for at least 8 h in a Hitachi F-2000 fluorometer as described previously (46). More detailed information about the ratiometric $Ca^{2+}$ measuring method is provided in the *SI Methods*.

**Microinjections.** Intracellular injections were carried out as described previously (7, 9, 10, 31). More detailed information is provided in the *SI Methods*.

**Proliferation Assays of Cultured T Cells.** Antigen-specific rat T cells ($T_{MBP}$ and $T_{OVA}$) were co-cultured for 48 h in 96-well plates (in DMEM 1% rat serum) with irradiated professional thymic APCs as previously described (45), in presence of specific or control antigen (10 $\mu$g/mL MBP or OVA) and BZ194 in DMSO or DMSO alone. Amplification of $T_{MBP\text{-}GFP}$ cells was measured by cytofluorometry. Their numbers were determined in relation to a known absolute number of added phycoerythrin-labeled plastic beads (Becton Dickinson). The amplification rate was calculated in relation to the $T_{GFP}$ cell numbers at day 0. Alternatively, [$^3$H]-2′-deoxy-thymidine ([$^3$H]dT; 2 Ci/mmol; Amersham) incorporation was used to evaluate proliferation. Radioactivity was determined as described (47). More detailed information about proliferation assays in rat T cells is provided in the *SI Methods*.

**Quantitative PCR and ELISAs.** Detailed information is provided in the *SI Methods*.

**ACKNOWLEDGMENTS.** The authors thank Sabine Kosin, Karin Weber and Martina Sölch for excellent technical assistance. We thank Markus Hammer and Hans-Dieter Volk (Charité-Universitätsmedizin, Berlin) for providing us with human taqman primers and probes. This work was supported by the Deutsche Forschungsgemeinschaft (SFB 455-A8 to A.F., SFB571-A1 to K.D., GU 360/7–1,7–2,7–3,7–5 to A.H.G.), the Gemeinnützige Hertie Foundation (Grant 1.01.1/04/010 and 1.01.1/07/005 to A.F. and A.H.G.), an Enterprise Development Grant from the University of Bath (to B.V.L.P), the Fonds zur Förderung der wissenschaftlichen Forschung (FWF; Grant P-14940 to M.H.), and the Wellcome Trust (Biomedical Research Collaboration Grant 068065 to B.V.L.P. and A.H.G.).

1. Feske S, et al. (2006) A mutation in Orai1 causes immune deficiency by abrogating CRAC channel function. *Nature* 441:179–185.
2. Vig M, et al. (2006) CRACM1 is a plasma membrane protein essential for store-operated $Ca^{2+}$ entry. *Science* 312:1220–1223.
3. Yeromin AV, et al. (2006) Molecular identification of the CRAC channel by altered ion selectivity in a mutant of Orai. *Nature* 443:226–229.
4. Peinelt C (2006) Amplification of CRAC current by STIM1 and CRACM1 (Orai1). *NatCell Biol* 8:771–773.
5. Streb H, Irvine RF, Berridge MJ, Schulz I (1983) Release of $Ca^{2+}$ from a nonmitochondrial intracellular store in pancreatic acinar cells by inositol-1,4,5-trisphosphate. *Nature* 306:67–69.
6. Guse AH, et al. (1999) Regulation of calcium signaling in T lymphocytes by the second messenger cyclic ADP-ribose. *Nature* 398:70–73.
7. Berg I, Potter BVL, Mayr GW, Guse AH (2000) Nicotinic acid adenine dinucleotide phosphate ($NAADP^+$) is an essential regulator of T-lymphocyte $Ca^{2+}$-signaling. *J Cell Biol* 150:581–588.
8. Gasser A, Bruhn S, Guse AH (2006) Second messenger function of nicotinic acid adenine dinucleotide phosphate revealed by an improved enzymatic cycling assay. *J BiolChem* 281:16906–16913.
9. Dammermann W, Guse AH (2005) Functional ryanodine receptor expression is required for NAADP-mediated local $Ca^{2+}$ signaling in T-lymphocytes. *J BiolChem* 280:21394–21399.
10. Langhorst MF, Schwarzmann N, Guse AH (2004) $Ca^{2+}$ release via ryanodine receptors and $Ca^{2+}$ entry: Major mechanisms in NAADP-mediated $Ca^{2+}$ signaling in T-lymphocytes. *Cell Signal* 16:1283–1289.
11. Lee HC, Aarhus R (1995) A derivative of NADP mobilizes calcium stores insensitive to inositol trisphosphate and cyclic ADP-ribose. *J BiolChem* 270:2152–2157.
12. Guse AH (2002) Cyclic ADP-ribose (cADPR) and nicotinic acid adenine dinucleotide phosphate (NAADP): Novel regulators of $Ca^{2+}$-signaling and cell function. *Curr Mol Med* 2:273–282.
13. Yamasaki M, Churchill GC, Galione A (2005) Calcium signalling by nicotinic acid adenine dinucleotide phosphate (NAADP). *FEBS J* 272:4598–4606.
14. Lee HC (2005) Nicotinic acid adenine dinucleotide phosphate (NAADP)-mediated calcium signaling. *J Biol Chem* 280:33693–33696.
15. Lee HC (2003) Calcium signaling: NAADP ascends as a new messenger. *Curr Biol* 13:186–188.
16. Rutter GA (2003) Calcium signalling: NAADP comes out of the shadows. *Biochem J* 373:3–4.
17. Guse AH, Lee HC (2008) NAADP: A universal $Ca^{2+}$ trigger. *Sci. Signal.* 1:re10.
18. Churchill GC, Galione A (2000) Spatial control of $Ca^{2+}$ signaling by nicotinic acid adenine dinucleotide phosphate diffusion and gradients. *J Biol Chem* 275:38687–38692.
19. Lee HC (2000) Functional visualization of the separate but interacting calcium stores sensitive to NAADP and cyclic ADP-ribose. *J Cell Sci* 113:4413–4420.
20. Masgrau R, Churchill GC, Morgan AJ, Ashcroft SJ, Galione A (2003) NAADP: A new second messenger for glucose-induced $Ca^{2+}$ responses in clonal pancreatic beta cells. *CurrBiol* 13:247–251.
21. Kinnear NP, Boittin FX, Thomas JM, Galione A, Evans AM (2004) Lysosome-sarcoplasmic reticulum junctions. A trigger zone for calcium signaling by nicotinic acid adenine dinucleotide phosphate and endothelin-1. *J BiolChem* 279:54319–54326.
22. Churchill GC, et al. (2002) NAADP mobilizes $Ca^{2+}$ from reserve granules, lysosome-related organelles, in sea urchin eggs. *Cell* 111:703–708.
23. Yamasaki M, et al. (2004) Organelle selection determines agonist-specific $Ca^{2+}$ signals in pancreatic acinar and beta cells. *J Biol Chem* 279:7234–7240.
24. Zhang F, Li PL (2007) Reconstitution and characterization of a nicotinic acid adenine dinucleotide phosphate (NAADP)-sensitive $Ca^{2+}$ release channel from liver lysosomes of rats. *J Biol Chem* 282:25259–25269.
25. Zhang F, Jin S, Yi F, Li PL (August 27, 2008) TRP-ML1 Functions as a lysosomal NAADP-sensitive Ca(2+) release channel in coronary arterial myocytes. *J Cell Mol Med*, 10.1111/j.1582-4934.2008.00486.x.
26. Hohenegger M, Suko J, Gscheidlinger R, Drobny H, Zidar A (2002) Nicotinic acid-adenine dinucleotide phosphate activates the skeletal muscle ryanodine receptor. *Biochem J* 367:423–431.
27. Mojzisova A, Krizanova O, Zacikova L, Kominkova V, Ondrias K (2001) Effect of nicotinic acid adenine dinucleotide phosphate on ryanodine calcium release channel in heart. *Pflugers Arch* 441:674–677.
28. Mitchell KJ, Lai FA, Rutter GA (2003) Ryanodine receptor type I and nicotinic acid adenine dinucleotide phosphate receptors mediate $Ca^{2+}$ release from insulin-containing vesicles in living pancreatic beta-cells (MIN6). *J Biol Chem* 278:11057–11064.
29. Gerasimenko JV, et al. (2003) NAADP mobilizes $Ca^{2+}$ from a thapsigargin-sensitive store in the nuclear envelope by activating ryanodine receptors. *J Cell Biol* 163:271–282.
30. Gerasimenko JV, Sherwood M, Tepikin AV, Petersen OH, Gerasimenko OV (2006) NAADP, cADPR, and $IP_3$ all release $Ca^{2+}$ from the endoplasmic reticulum and an acidic store in the secretory granule area. *J Cell Sci* 119:226–238.
31. Steen M, Kirchberger T, Guse AH (2007) NAADP mobilizes calcium from the endoplasmic reticular $Ca^{2+}$ store in T lymphocytes. *J BiolChem* 282:18864–18871.
32. Tanna B, Welch W, Ruest L, Sutko JL, Williams AJ (2006) The interaction of an impermeant cation with the sheep cardiac RyR channel alters ryanoid association. *Mol Pharmacol* 69:1990–1997.
33. Lee HC, Aarhus R (1997) Structural determinants of nicotinic acid adenine dinucleotide phosphate important for its calcium-mobilizing activity. *J Biol Chem* 272:20378–20383.
34. Dowden J, et al. (2006) Cell-permeant small-molecule modulators of NAADP-mediated $Ca^{2+}$ release. *Chem Biol* 13:659–665.
35. Imagawa T, Smith JS, Coronado R, Campbell KP (1987) Purified ryanodine receptor from skeletal muscle sarcoplasmic reticulum is the $Ca^{2+}$-permeable pore of the calcium release channel. *J Biol Chem* 262:16636–16643.
36. Pessah IN, Francini AO, Scales DJ, Waterhouse AL, Casida JE (1986) Calcium-ryanodine receptor complex. Solubilization and partial characterization from skeletal muscle junctional sarcoplasmic reticulum vesicles. *J Biol Chem* 261:8643–8648.
37. Chu A, Díaz-Muñoz M, Hawkes MJ, Brush K, Hamilton SL (1990) Ryanodine as a probe for the functional state of the skeletal muscle sarcoplasmic reticulum calcium release channel. *Mol Pharmacol* 37:735–741.
38. Schwarzmann N, Kunerth S, Weber K, Mayr GW, Guse AH (2002) Knock-down of the Type 3 ryanodine receptor impairs sustained $Ca^{2+}$ signaling via the T cell receptor/CD3 Complex. *J Biol Chem* 277:50636–50642.
39. Guse AH, Goldwich A, Weber K, Mayr GW (1995) Non-radioactive, isomer-specific inositol phosphate mass determinations: high-performance liquid chromatography-micro-metal-dye detection strongly improves speed and sensitivity of analyses from cells and micro-enzyme assays. *J Chromatogr B* 672:189–198.
40. da Silva CP, Guse AH (2000) Intracellular $Ca^{2+}$ release mechanisms: Multiple pathways having multiple functions within the same cell type? *Biochim Biophys Acta* 1498:122–133.
41. Timmerman LA, Clipstone NA, Ho SN, Northrop JP, Crabtree GR (1996) Rapid shuttling of NF-AT in discrimination of $Ca^{2+}$ signals and immunosuppression. *Nature* 383:837–840.
42. Klinger M, et al. (1999) Suramin and suramin analogs activate skeletal muscle ryanodine receptor via a calmodulin binding site. *Mol Pharmacol* 55:462–472.
43. Wolner I, Kassack MU, Ullmann H, Karel A, Hohenegger M (2005) Use-dependent inhibition of the skeletal muscle ryanodine receptor by the Suramin analogue NF676. *Br J Pharmacol* 146:525–533.
44. Guse AH, Roth E, Emmrich F (1993) Intracellular $Ca^{2+}$ pools in Jurkat T-lymphocytes. *Biochem J* 291:447–451.
45. Flügel A, Willem M, Berkowicz T, Wekerle H (1999) Gene transfer into $CD4^+$ T lymphocytes: Green fluorescent protein engineered, encephalitogenic T cells used to illuminate immune responses in the brain. *Nature Med* 5:843–847.
46. Guse AH, et al. (2005) A minimal structural analogue of cyclic ADP-ribose: synthesis and calcium release activity in mammalian cells. *J Biol Chem* 280:15952–15959.
47. Flügel A, et al. (2001) Migratory activity and functional changes of green fluorescent effector T cells before and during experimental autoimmune encephalomyelitis. *Immunity* 14:547–560.